

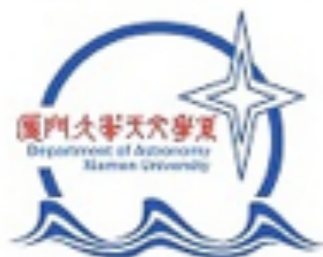
Nucleon Spin Structure Evolution and Spin Dependent Dark Matter-Nucleon Interaction

Feng Huang (黃峰)

Licheng Yang (杨里程)

Shaoyang Jia (贾少阳)

Taotao Fang (方陶陶)

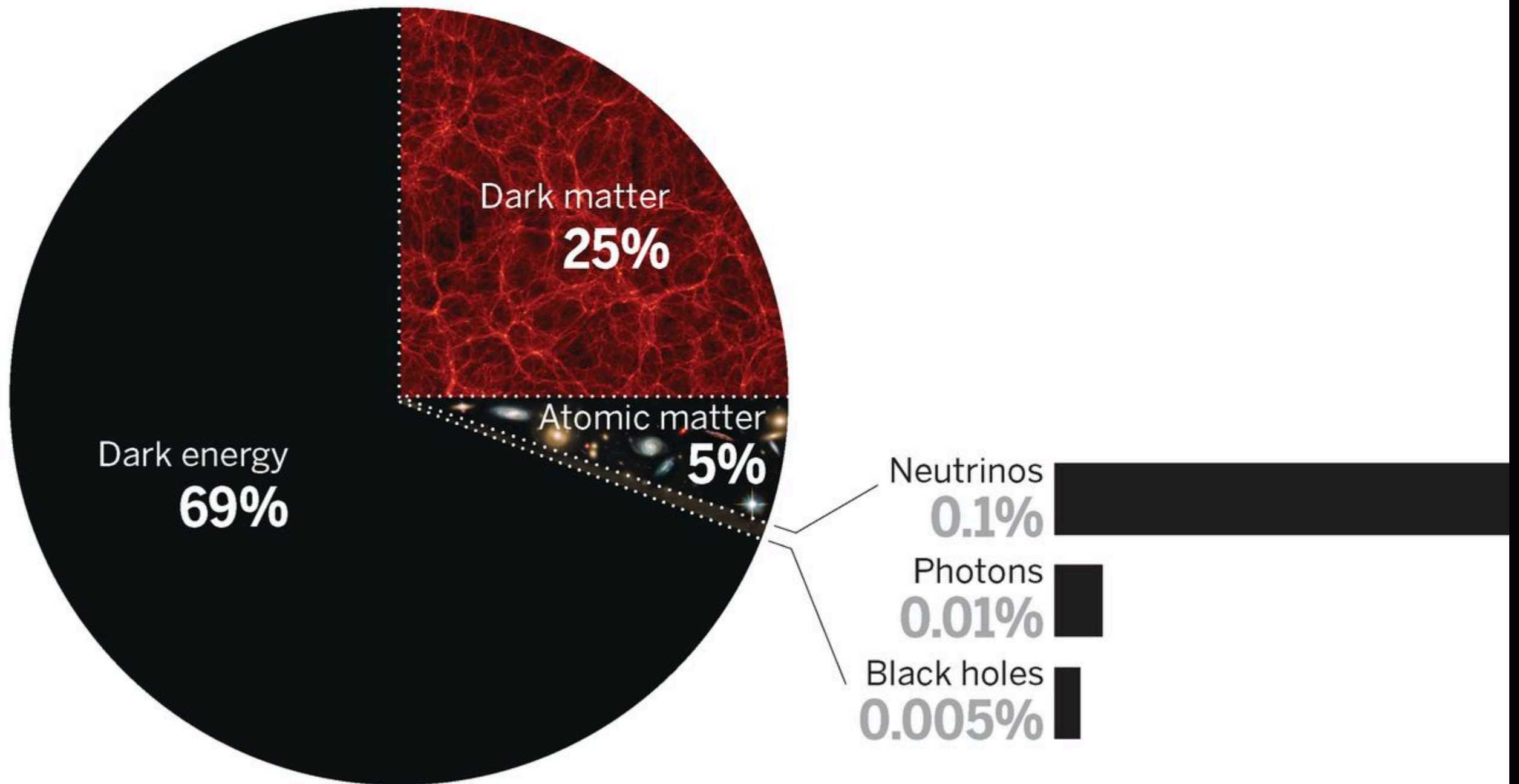


廈門大學天文學系

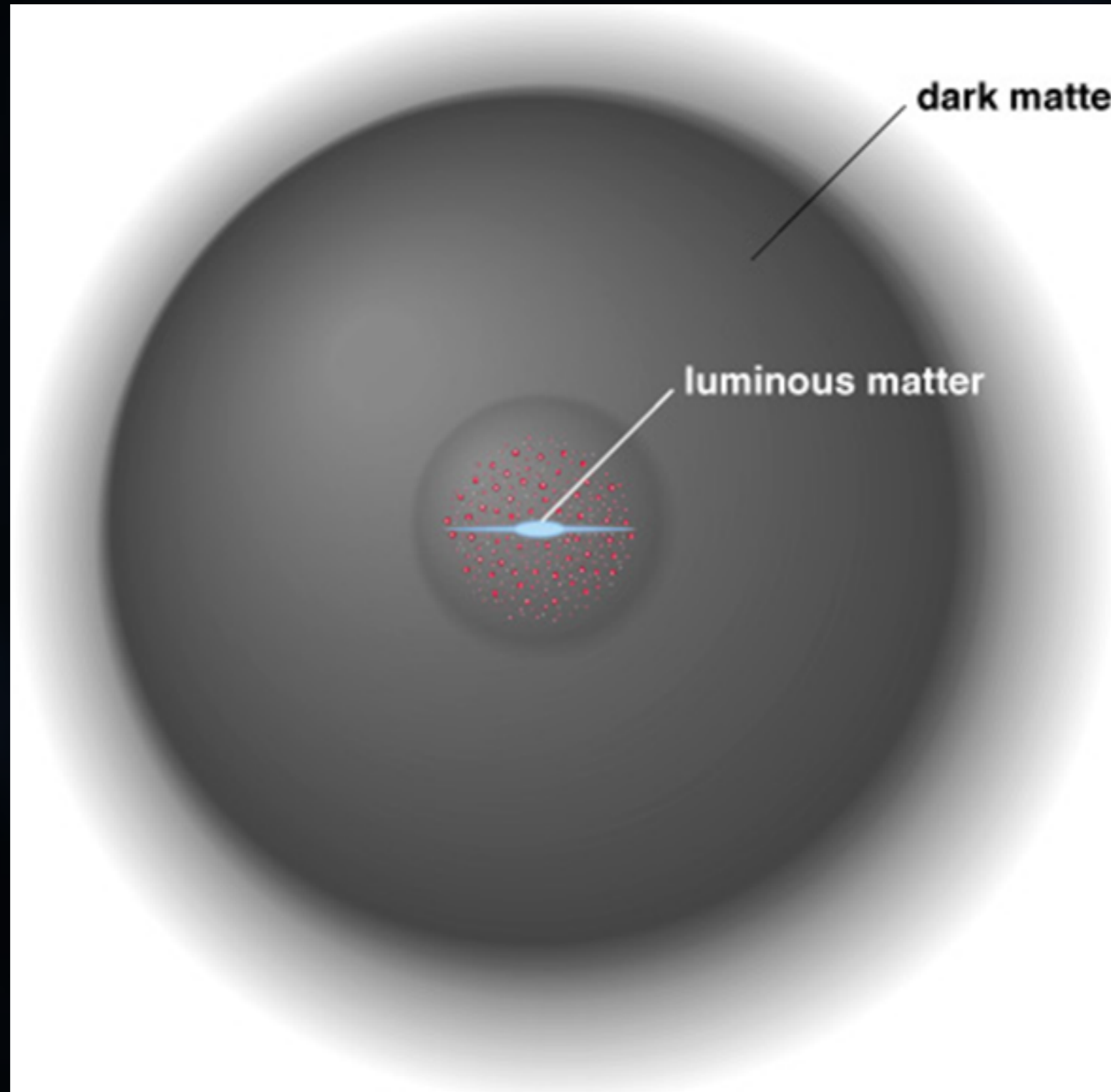
2019-12-09

The multiple components that compose our universe

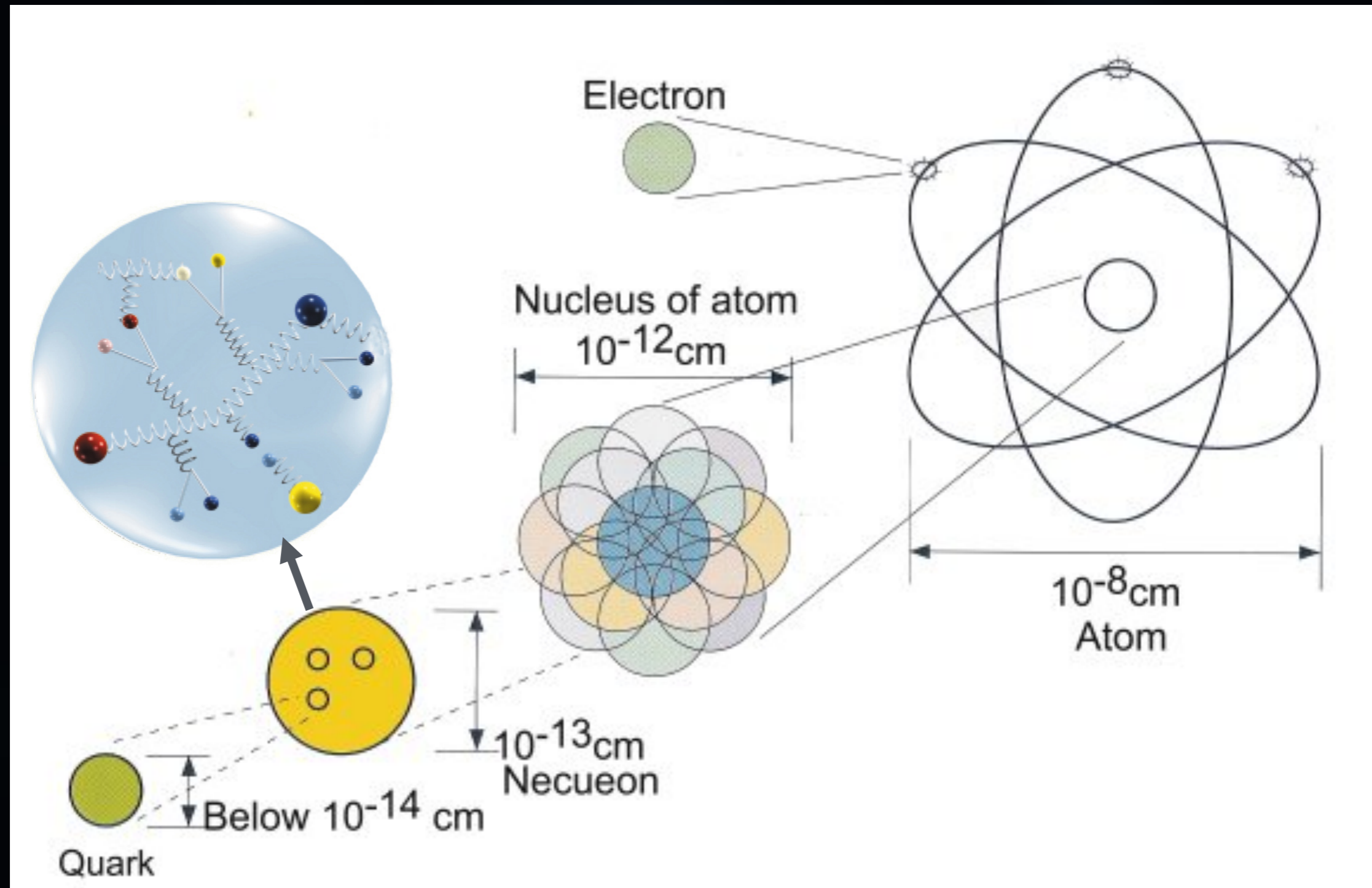
Current composition (as the fractions evolve with time)



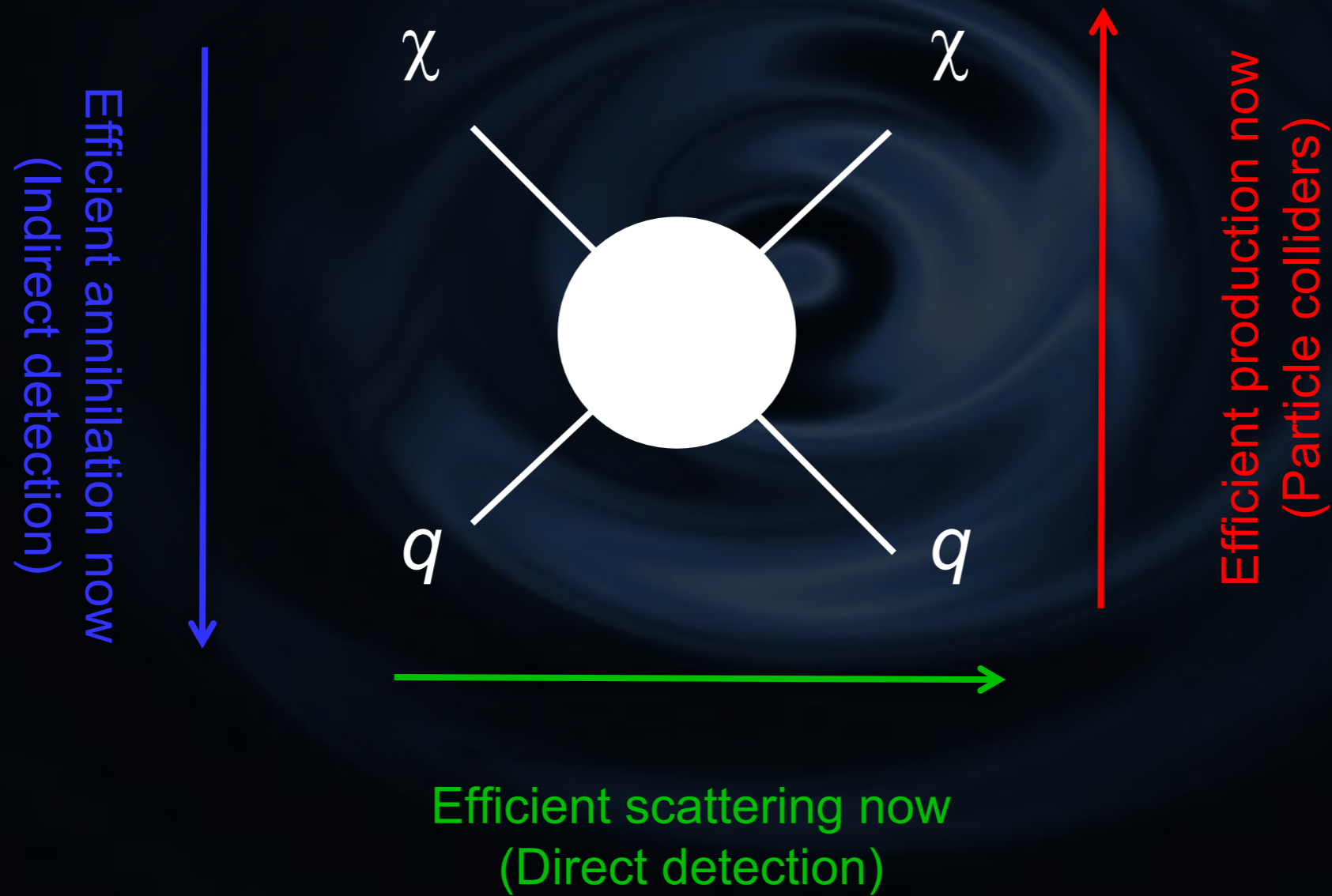
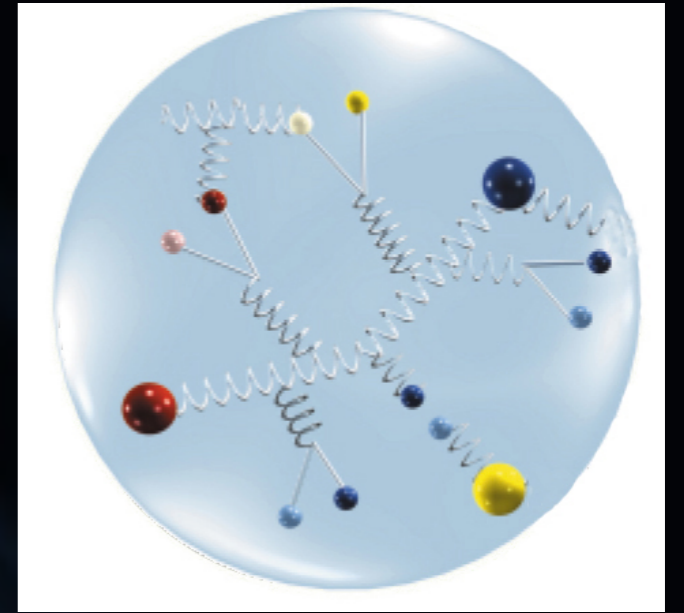
Dark Matter



Baryon Matter



DM-Nucleon(Quark)



DM-Nucleon Interaction : Effective Theory

Spin Independent

$$L = f_q (\bar{\chi}\chi) \cdot (\bar{q}q) + d_q (\bar{\chi}\gamma^\mu \gamma^5 \chi) \cdot (\bar{q}\gamma_\mu \gamma^5 q) + \dots$$

Spin Dependent

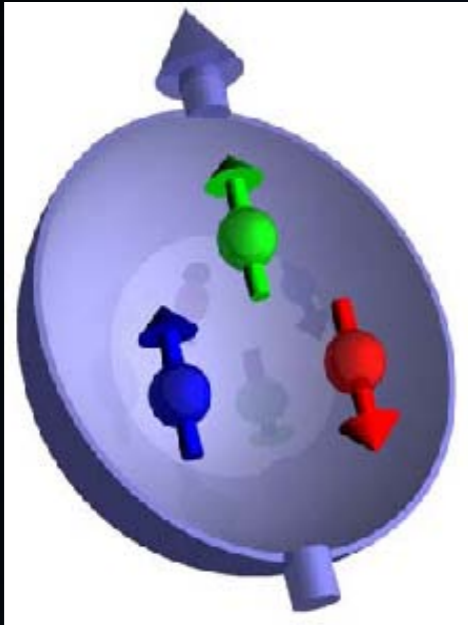
$$\sigma_{\chi p}^{\text{SD}} = \frac{3\mu_{\chi p}^2}{\pi} |G_a^p|^2, \quad \sigma_{\chi n}^{\text{SD}} = \frac{3\mu_{\chi n}^2}{\pi} |G_a^n|^2$$

$$G_a^N = \sum_{q=u,d,s} (\Delta q)_N \left(\frac{g_{Z\chi\chi} g_{Zqq}}{m_Z^2} + \frac{1}{8} \sum_{k=1}^6 \frac{g_{L\bar{q}_k\chi q}^2 + g_{R\bar{q}_k\chi q}^2}{m_{\bar{q}_k}^2} \right)$$

Quark Spin in Nucleon

Nucleon Spin Structure

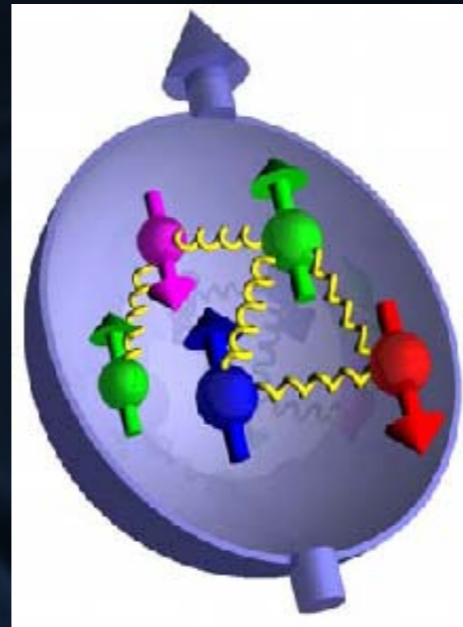
1980's



Naive parton model
3 valence quarks

$$\frac{1}{2} = \frac{1}{2}(\Delta u + \Delta d)$$

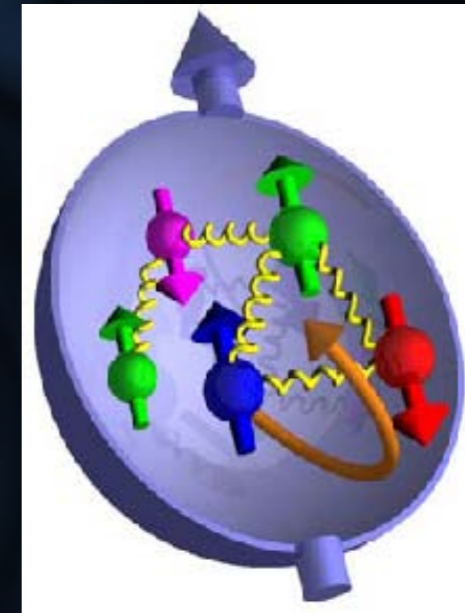
1990's



QCD: contributions from
sea quarks and gluons

$$\frac{1}{2} = \frac{1}{2} \underbrace{(\Delta u + \Delta d + \Delta s)}_{\Delta \Sigma} + \Delta G + L$$

2000's



.. and orbital angular
momentum

nucleon spin is 1/2

quark spin component

in near zero momentum transfer region?

Nucleon Spin Structure in Low Q

Lattice QCD

• **Phenomenological model**

• **Experiment data GeV^2**

Evolution?

the scale of 0.01GeV^2

Nucleon Spin Structure Evolution

Our Model:

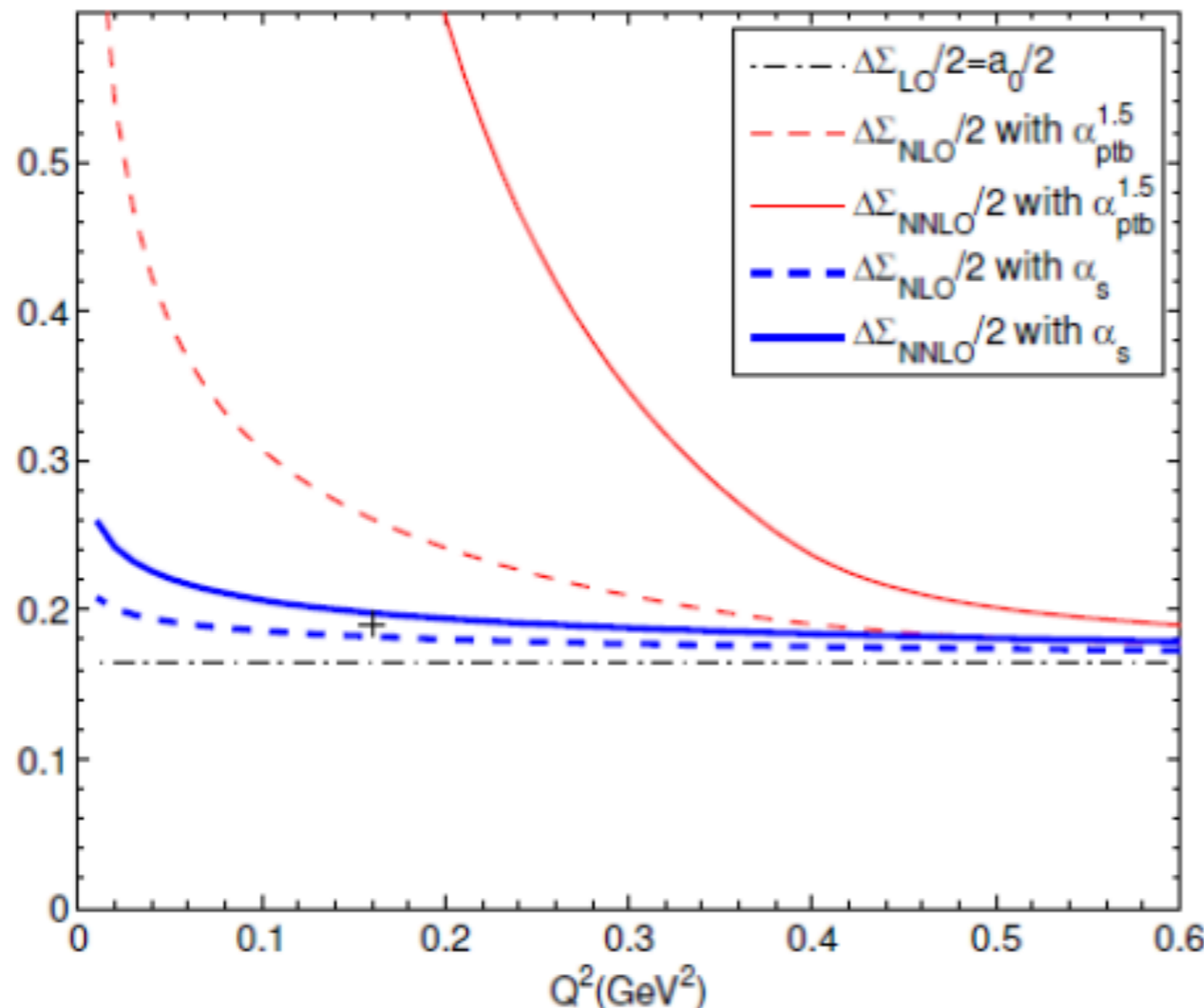
- Step 1: Expand the Nucleon property in α_s
- Step 2: Find the scale dependency of α_s



Converge in the low energy region

Nucleon Spin Structure Evolution

$$\Delta\Sigma(Q^2) = \Delta\Sigma(\mu^2) \exp \left\{ \int_{Q^2}^{\mu^2} \left(8n_f \left(\frac{\alpha_s(Q^2)}{4\pi} \right)^2 + \left(200n_f - \frac{16}{9}n_f^2 \right) \left(\frac{\alpha_s(Q^2)}{4\pi} \right)^3 \right) \frac{dQ^2}{Q^2} \right\}. \quad (10)$$

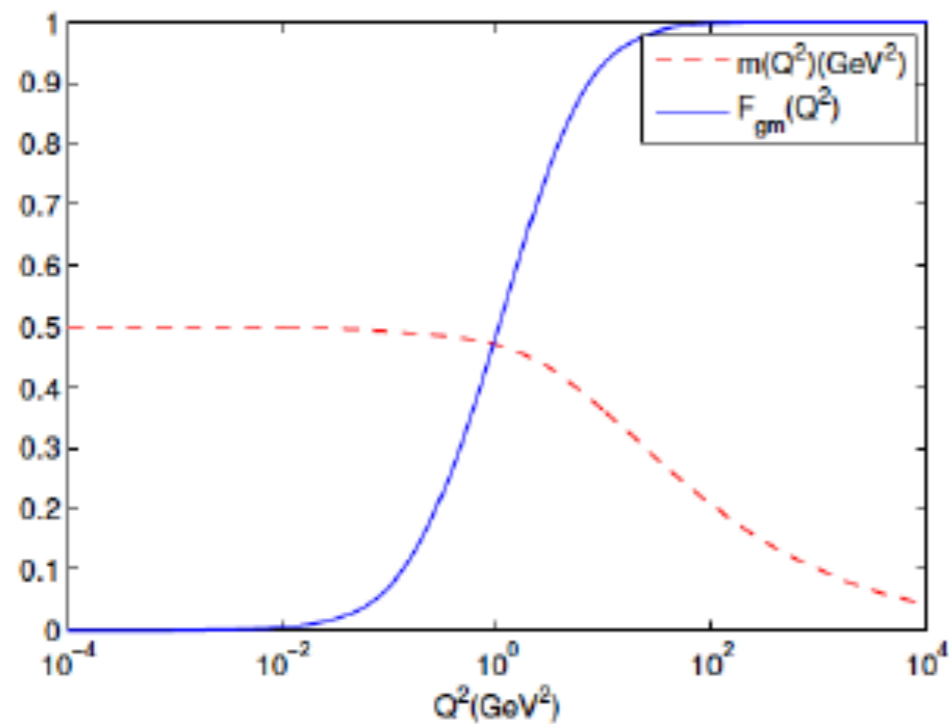


(1): perturbatively expand to what kind of order

(2): How does the coupling constant evolve with the energy scale Q^2

QCD coupling constant α_s

$$\beta(\alpha_s) = -\alpha_s^2(\beta_0 + \beta_1\alpha_s + \beta_2\alpha_s^2 + \dots)$$



$$Q^2 \frac{d\alpha_s}{dQ^2} = \beta(\alpha_s).$$



$$Q^2 \frac{d\alpha_s}{dQ^2} = \beta_{ptb}(\alpha_s) F_{gm}(Q^2),$$

FIG. 2. Scale Dependence of m and F_{gm} ; Solid line for correction factor, and dashed line for effective gluon mass in unit of GeV.

$$F_{gm}(Q^2) = \frac{Q^2}{4m^2(Q^2) + Q^2} \left(1 + 4 \frac{dm^2(Q^2)}{dQ^2} \right)$$

$$m^2(Q^2) = \frac{m_0^4}{Q^2 + m_0^2} \left[\ln \left(\frac{Q^2 + 2m_0^2}{\Lambda_{\text{QCD}}} \right) / \ln \left(\frac{2m_0^2}{\Lambda_{\text{QCD}}^2} \right) \right]^3$$

$$Q^2 \frac{d\alpha_s}{dQ^2} = \beta_{ptb}(\alpha_s) F_{gm}(Q^2),$$

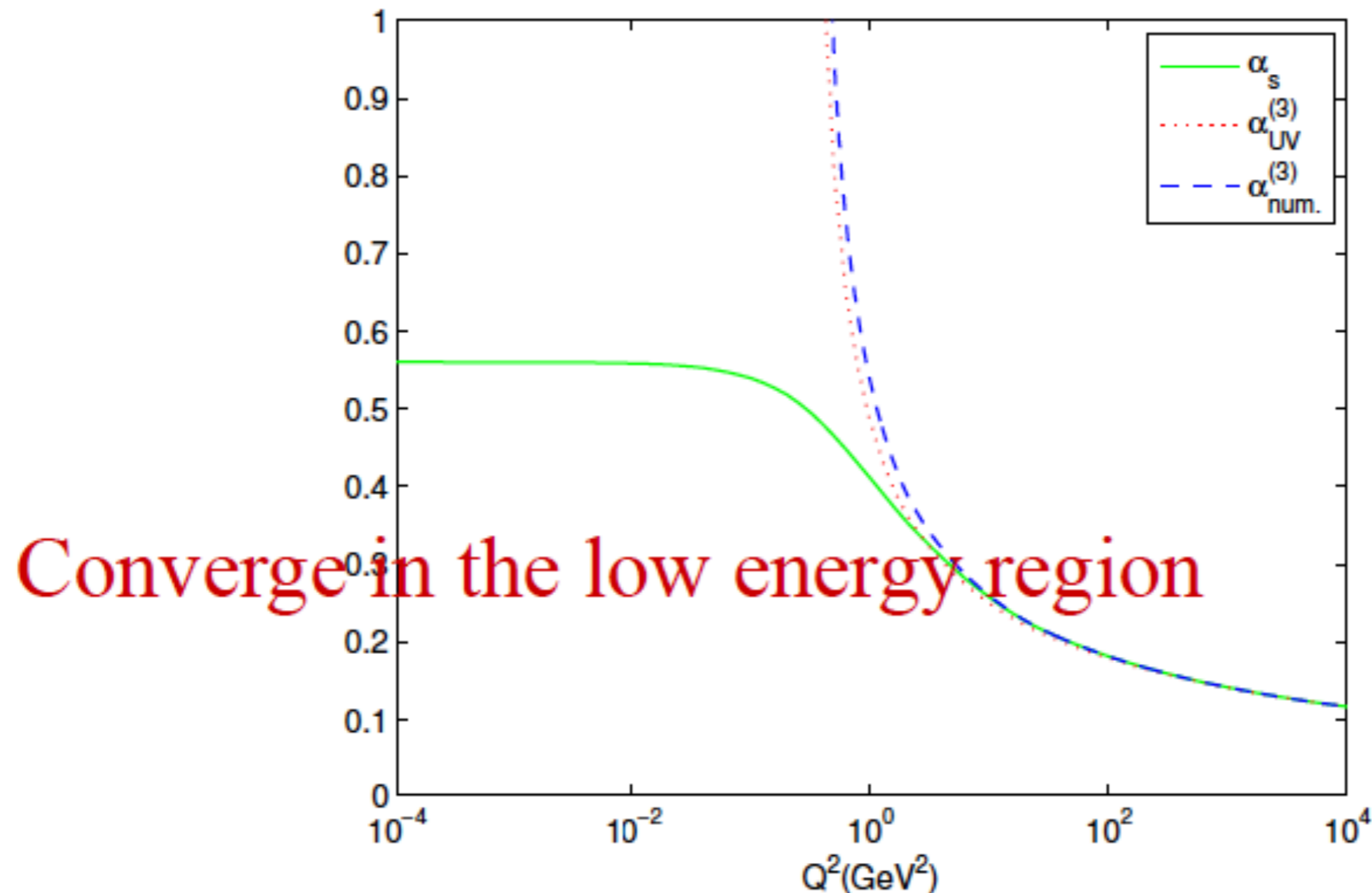
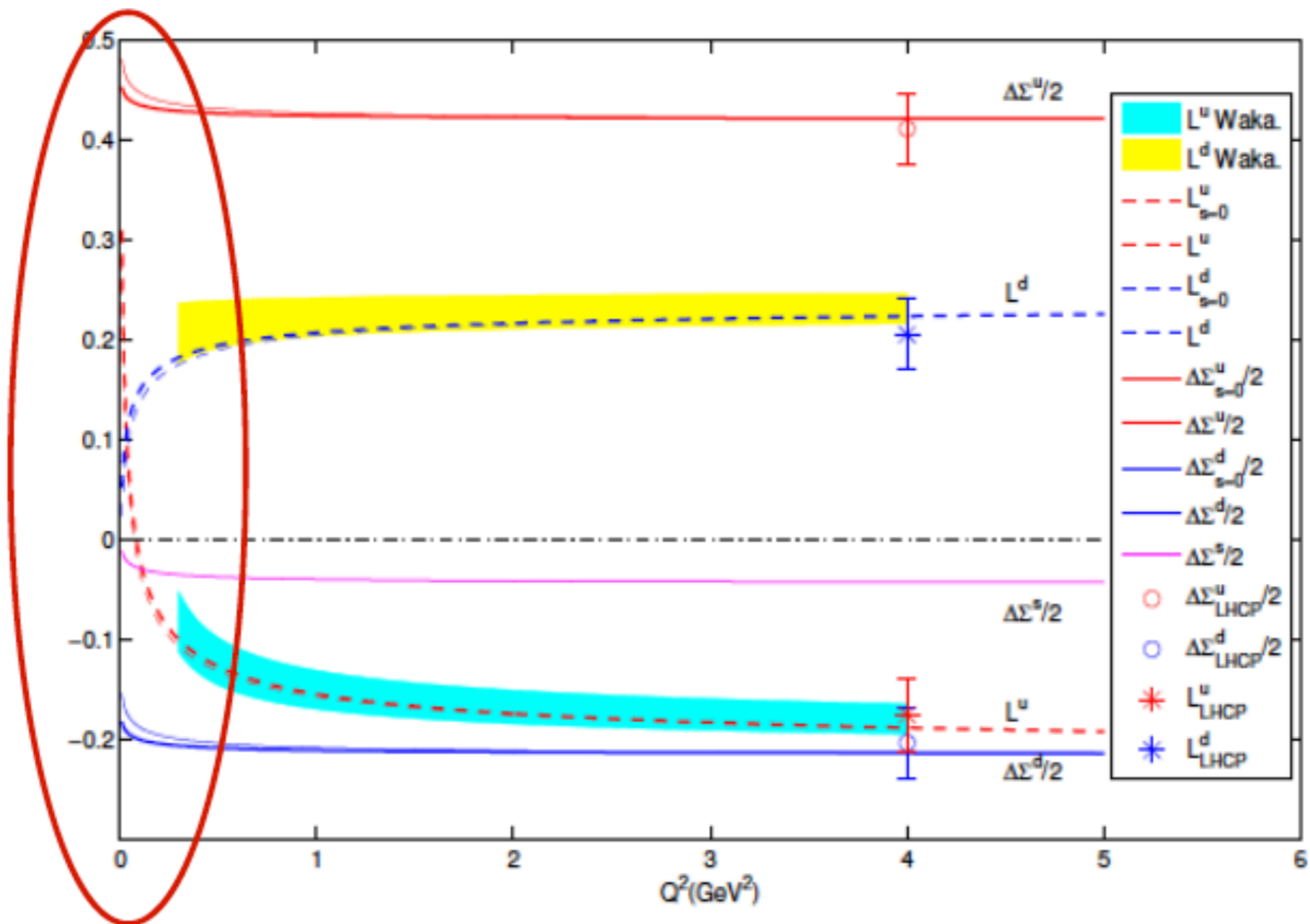


FIG. 1. Green solid line: numerical solution to Eq. (8) with four-loop β_{ptb} . Red dotted line: running coupling obtained by three-loop version of Eq. (B1). Blue dashed line: numerical solution to three-loop QCD beta function. All curves are normalized at $Q^2 = M_{Z_0}^2$.

Nucleon Spin Structure Evolution

$$\frac{1}{2} = \frac{1}{2} \underbrace{(\Delta u + \Delta d + \Delta s)}_{\Delta\Sigma} + \Delta G + L$$



DM-Nucleon Interaction : Effective Theory

Spin Independent

$$L = f_q (\bar{\chi}\chi) \cdot (\bar{q}q) + d_q (\bar{\chi}\gamma^\mu \gamma^5 \chi) \cdot (\bar{q}\gamma_\mu \gamma^5 q) + \dots$$

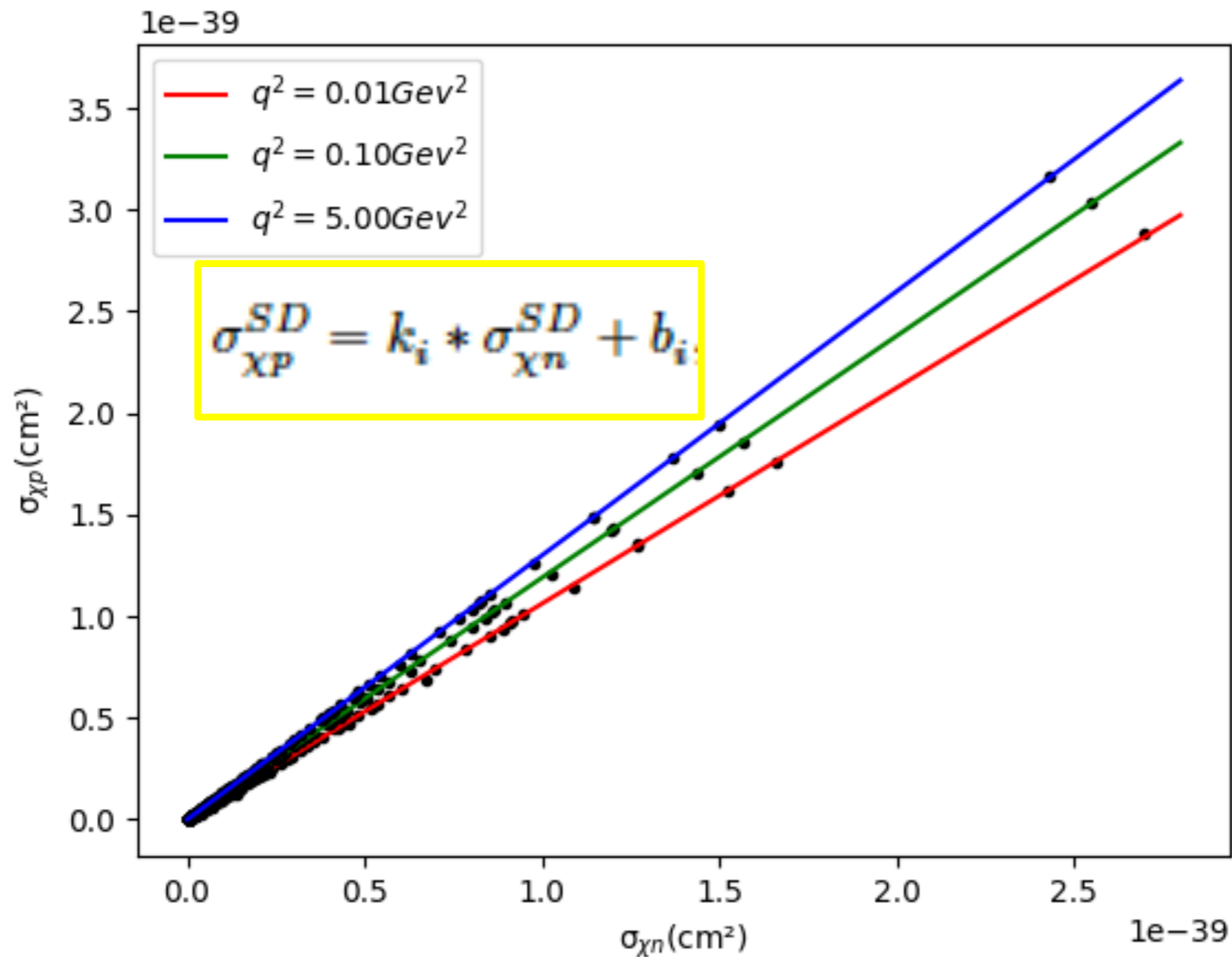
Spin Dependent

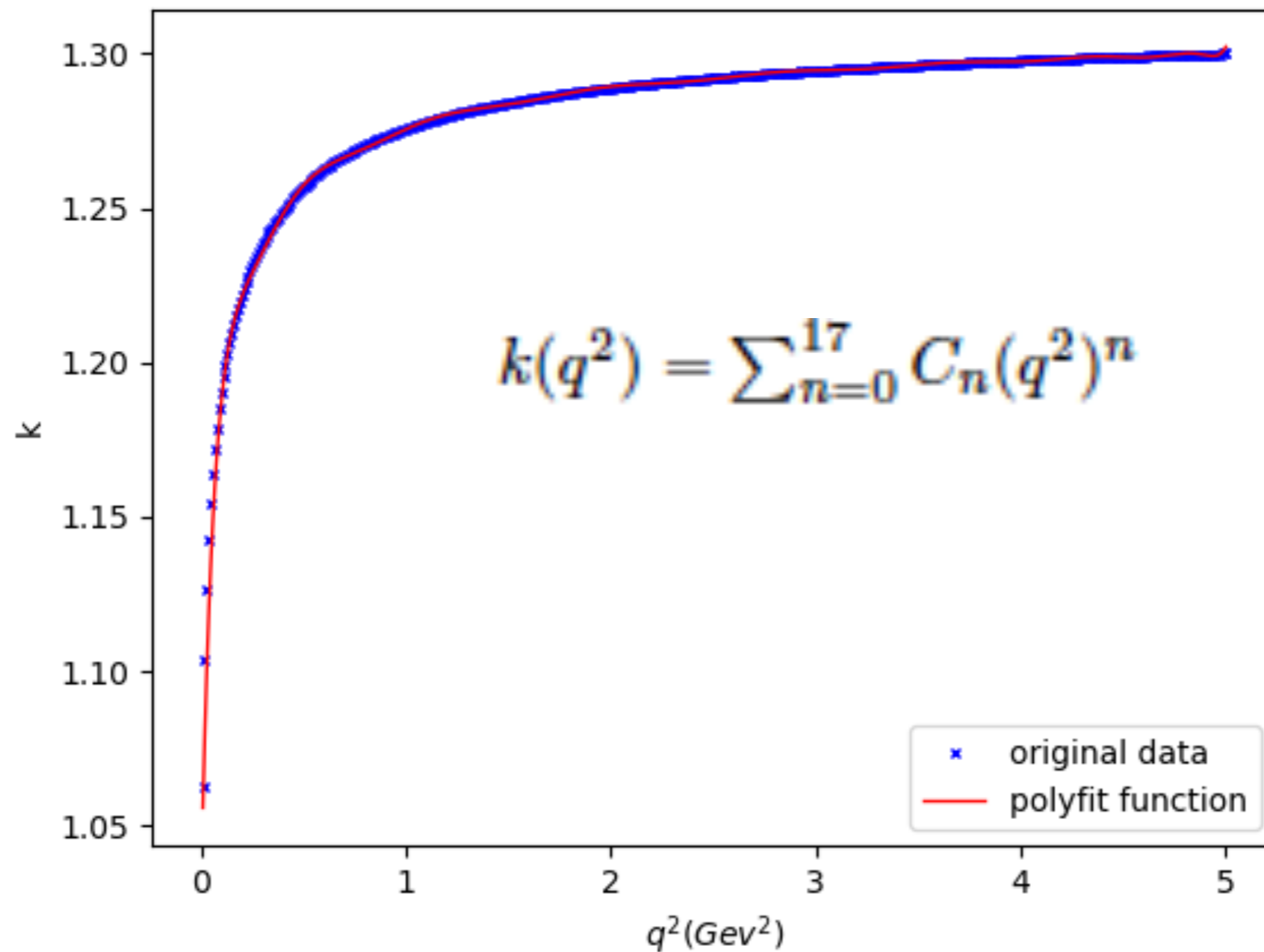
$$\sigma_{\chi p}^{\text{SD}} = \frac{3\mu_{\chi p}^2}{\pi} |G_a^p|^2, \quad \sigma_{\chi n}^{\text{SD}} = \frac{3\mu_{\chi n}^2}{\pi} |G_a^n|^2$$

$$G_a^N = \sum_{q=u,d,s} (\Delta q)_N \left(\frac{g_{Z\chi\chi} g_{Zqq}}{m_Z^2} + \frac{1}{8} \sum_{k=1}^6 \frac{g_{L\bar{q}_k\chi q}^2 + g_{R\bar{q}_k\chi q}^2}{m_{\bar{q}_k}^2} \right)$$

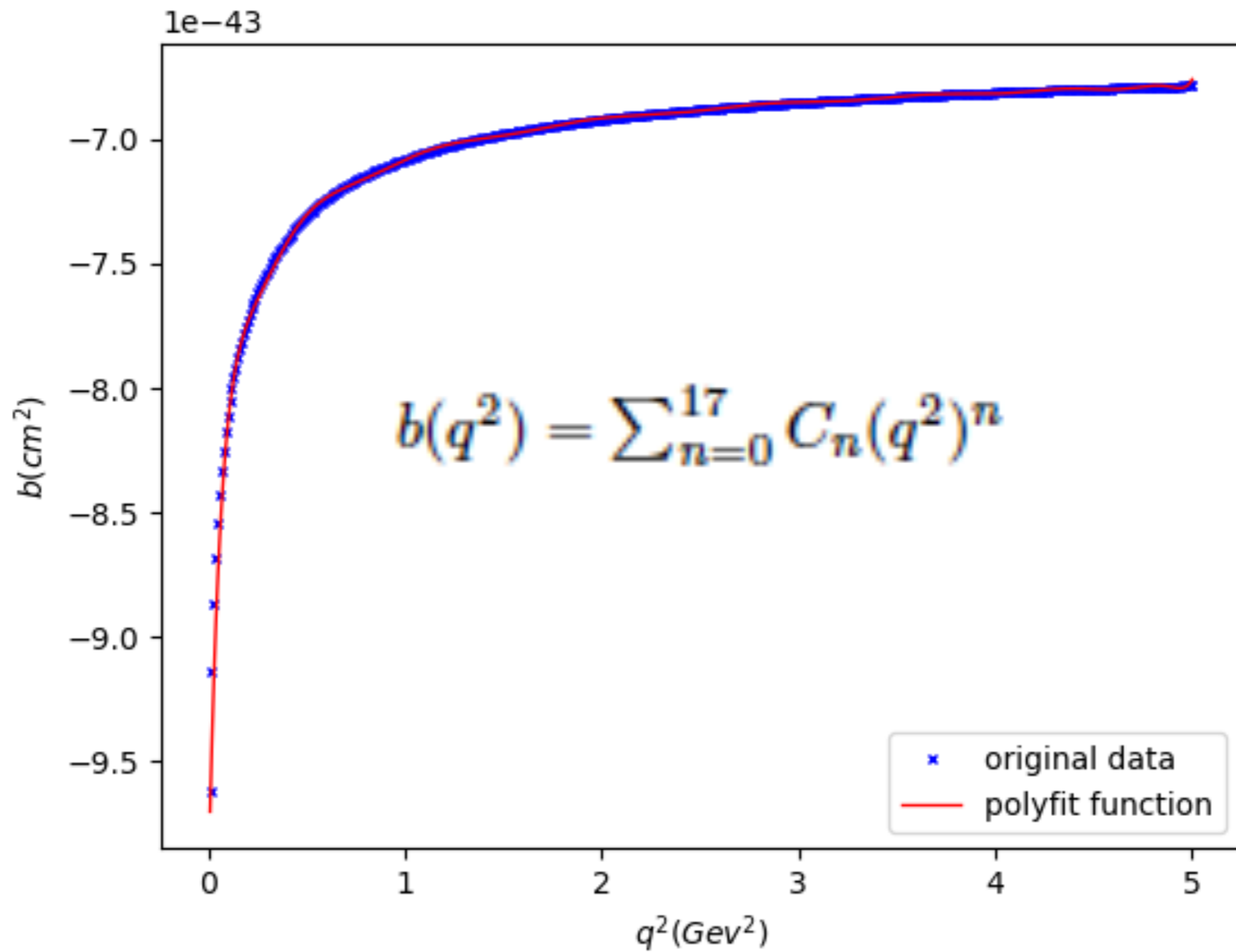
Quark Spin in Nucleon

$\sigma_{\chi p}^{SD} - \sigma_{\chi n}^{SD}$ Correlation





$x = q^2$	1	x	x^2	x^3	x^4	x^5
c_n	1.053	2.723	-20.099	88.307	-244.587	454.003
$x = q^2$	x^6	x^7	x^8	x^9	x^{10}	x^{11}
c_n	-591.378	558.537	-391.153	206.021	-82.194	24.845
$x = q^2$	x^{12}	x^{13}	x^{14}	x^{15}	x^{16}	x^{17}
c_n	-5.649	0.95	-0.114	9.352×10^{-3}	-4.635×10^{-4}	1.052×10^{-5}



$x = q^2$	1	x	x^2	x^3	x^4	x^5
c_n	-9.733×10^{-43}	3.208×10^{-42}	-2.356×10^{-41}	1.033×10^{-40}	-2.857×10^{-40}	5.299×10^{-40}
$x = q^2$	x^6	x^7	x^8	x^9	x^{10}	x^{11}
c_n	-6.899×10^{-40}	6.512×10^{-40}	-4.559×10^{-40}	2.401×10^{-40}	-9.575×10^{-41}	2.894×10^{-41}
$x = q^2$	x^{12}	x^{13}	x^{14}	x^{15}	x^{16}	x^{17}
c_n	-6.578×10^{-42}	1.106×10^{-42}	-1.333×10^{-43}	1.089×10^{-44}	-5.394×10^{-46}	1.224×10^{-47}

$$\frac{d\sigma_{WN}}{dE_R} = \frac{m_N}{2m_r^2 v^2} \sigma_{SD}(q) \quad E_R = \frac{q^2}{2m_N}$$

$$\sigma_{SD}(q) = \frac{32m_r^2 G_F^2}{2J+1} [a_p^2 S_{pp}(q) + a_p a_n S_{pn}(q) + a_n^2 S_{nn}(q)]$$

$$\sigma_{\chi p,n} = \frac{24}{\pi} G_F^2 \mu_{\chi p,n}^2 a_{\chi p,n}^2$$

	$\langle S_p \rangle$	$\langle S_n \rangle$	$\langle S_p \rangle$	$\langle S_n \rangle$
Experiment	^{129}Xe		^{131}Xe	
Bonn A	0.028	0.359	-0.009	-0.227
Nijmegen II	0.0128	0.300	-0.012	-0.217

J. Menendez: Table 1 @ PhysRevD.86.103511

TABLE I. Fits to the structure factors S_{00} , S_{11} , and S_{01} for spin-dependent WIMP elastic scattering off ^{129}Xe and ^{131}Xe nuclei, including 1b and 2b currents as in Figs. 2 and 3. For the 1b + 2b current results, both the central value of the theoretical error band was used for the fits (first rows) and the limits of the band (second rows). The fitting function of the dimensionless variable $u = p^2 b^2 / 2$ is $S_{ij}(u) = e^{-u} \sum_{n=0}^9 c_{ij,n} u^n$. The rows give the coefficients $c_{ij,n}$ of the u^n terms in the polynomial.

^{129}Xe					
$u = p^2 b^2 / 2, b = 2.2853 \text{ fm}$					
$e^{-u} \times$	S_{00}	S_{11} (1b)	S_{11} (1b + 2b)	S_{01} (1b)	S_{01} (1b + 2b)
1	0.054 731	0.048 192	0.02 933	-0.102 732	-0.0 796 645
u	-0.146 897	-0.148 361	-0.0905 396	0.297 105	0.231 997
u^2	0.182 479	0.202 347	0.122 783	-0.387 513	-0.304 198
u^3	-0.128 112	-0.151 853	-0.0912 046	0.281 816	0.222 024
u^4	0.0 539 978	0.0 674 284	0.0 401 076	-0.122 388	-0.096 693
u^5	-0.0 133 335	-0.0 179 342	-0.010 598	0.0 317 668	0.0 251 835
u^6	0.00 190 579	0.00 286 368	0.00 168 737	-0.00 492 337	-0.00 392 356
u^7	$-1.48 373 \times 10^{-4}$	$-2.65 795 \times 10^{-4}$	$-1.56 768 \times 10^{-4}$	$4.39 836 \times 10^{-4}$	$3.53 343 \times 10^{-4}$
u^8	$5.11 732 \times 10^{-6}$	$1.29 656 \times 10^{-5}$	$7.69 202 \times 10^{-6}$	$-2.02 852 \times 10^{-5}$	$-1.65 058 \times 10^{-5}$
u^9	$-2.06 597 \times 10^{-8}$	$-2.47 418 \times 10^{-7}$	$-1.48 874 \times 10^{-7}$	$3.46 755 \times 10^{-7}$	$2.88 576 \times 10^{-7}$
$e^{-u} \times$	S_{11} (1b + 2b band)		S_{01} (1b + 2b band)		
1	0.0 360 513	0.0 226 064	-0.0 888 962	-0.070 431	
u	-0.1 10 705	-0.0 703 558	0.257 562	0.20 644	
u^2	0.150 026	0.0 954 932	-0.336 681	-0.271 749	
u^3	-0.1 11 714	-0.0 706 386	0.245 328	0.198 772	
u^4	0.0 493 115	0.0 308 683	-0.106 746	-0.0 866 783	
u^5	-0.0 130 745	-0.00 810 917	0.0 277 603	0.0 226 217	
u^6	0.00 208 705	0.00 128 522	-0.00 431 334	-0.00 353 705	
u^7	$-1.94 174 \times 10^{-4}$	$-1.19 086 \times 10^{-4}$	$3.86 604 \times 10^{-4}$	$3.20 472 \times 10^{-4}$	
u^8	$9.52 295 \times 10^{-6}$	$5.84 562 \times 10^{-6}$	$-1.79 013 \times 10^{-5}$	$-1.51 335 \times 10^{-5}$	
u^9	$-1.83 523 \times 10^{-7}$	$-1.13 885 \times 10^{-7}$	$3.06 893 \times 10^{-7}$	$2.70 785 \times 10^{-7}$	

$$^{131}\text{Xe}$$

$$u = p^2 b^2 / 2, b = 2.2905 \text{ fm}$$

$e^{-u} \times$	S_{00}	$S_{11} (1b)$	$S_{11} (1b + 2b)$	$S_{01} (1b)$	$S_{01} (1b + 2b)$
1	0.0417889	0.0368132	0.022446	-0.0784478	-0.0608808
u	-0.111171	-0.118361	-0.0733931	0.230484	0.181473
u^2	0.171966	0.176773	0.110509	-0.343106	-0.272533
u^3	-0.133219	-0.137987	-0.0868752	0.263525	0.211776
u^4	0.0633805	0.063821	0.0405399	-0.120946	-0.0985956
u^5	-0.0178388	-0.0176743	-0.0113544	0.0331754	0.027438
u^6	0.00282476	0.00287653	0.00187572	-0.00528724	-0.0044424
u^7	-2.31681×10^{-4}	-2.63605×10^{-4}	-1.75285×10^{-4}	4.6475×10^{-4}	3.97619×10^{-4}
u^8	7.78223×10^{-6}	1.23239×10^{-5}	8.40043×10^{-6}	-2.00407×10^{-5}	-1.74758×10^{-5}
u^9	-4.49287×10^{-10}	-2.17839×10^{-7}	-1.53632×10^{-7}	2.90375×10^{-7}	2.55979×10^{-7}

$e^{-u} \times$	$S_{11} (1b + 2b \text{ band})$		$S_{01} (1b + 2b \text{ band})$	
1	0.0275713	0.0173191	-0.067911	-0.0538485
u	-0.0891521	-0.0576174	0.20071	0.162246
u^2	0.134094	0.0868883	-0.301325	-0.24379
u^3	-0.105277	-0.0684403	0.233566	0.190041
u^4	0.0490864	0.0319771	-0.108494	-0.0887141
u^5	-0.0137279	-0.00897632	0.0301064	0.0247694
u^6	0.00226103	0.00148964	-0.00485087	-0.0040324
u^7	-2.10252×10^{-4}	-1.40246×10^{-4}	4.30628×10^{-4}	3.64368×10^{-4}
u^8	1.0004×10^{-5}	6.79325×10^{-6}	-1.86527×10^{-5}	-1.62836×10^{-5}
u^9	-1.80793×10^{-7}	-1.26396×10^{-7}	2.63842×10^{-7}	2.48126×10^{-7}

$$\frac{d\sigma_{WN}}{dE_R} = \frac{m_N}{2m_r^2 v^2} \sigma_{SD}(q) \quad E_R = \frac{q^2}{2m_N}$$

$$\sigma_{SD}(q) = \frac{32m_r^2 G_F^2}{2J+1} [a_p^2 S_{pp}(q) + a_p a_n S_{pn}(q) + a_n^2 S_{nn}(q)]$$

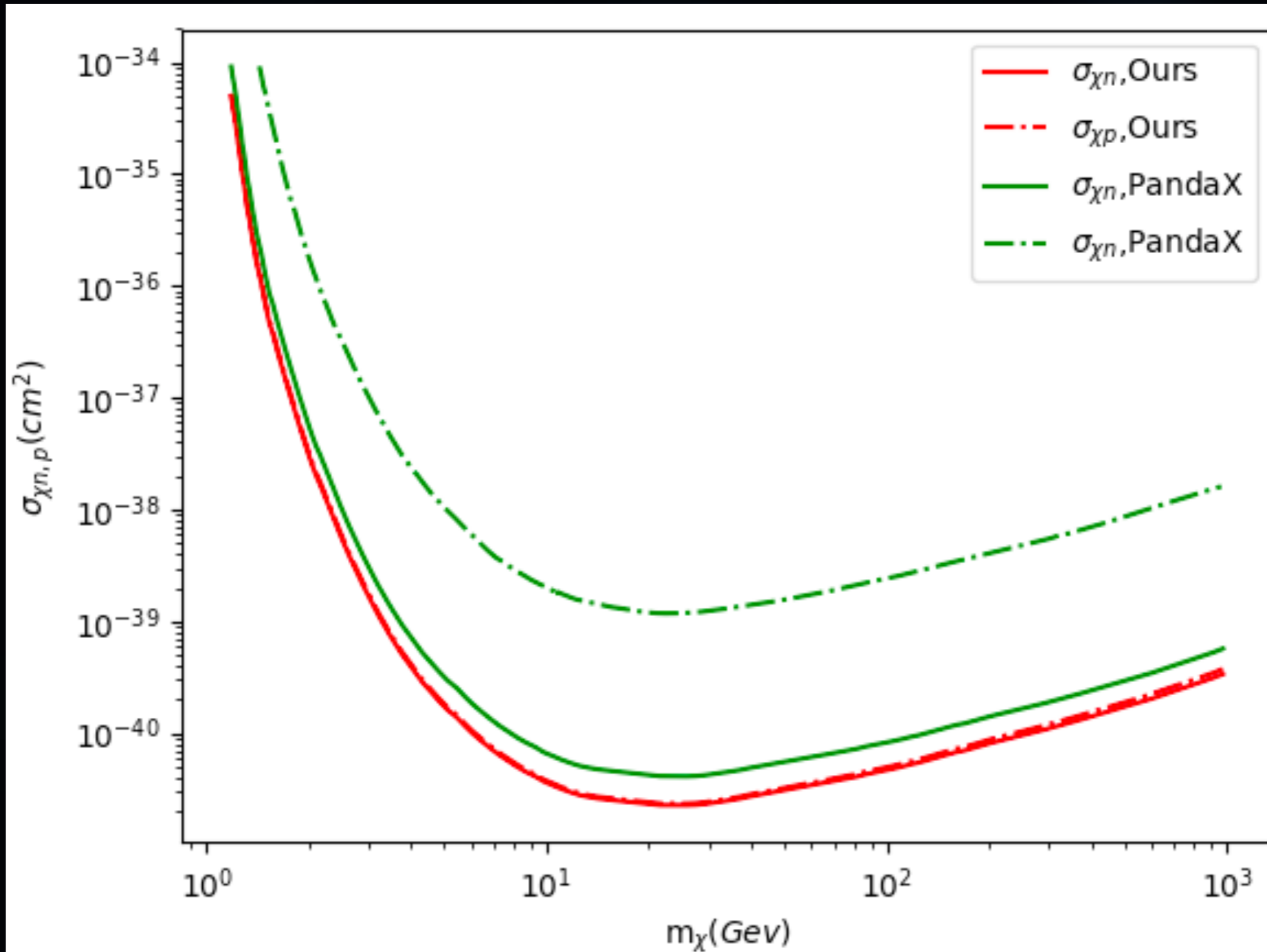
$$\sigma_{\chi p,n} = \frac{24}{\pi} G_F^2 \mu_{\chi p,n}^2 a_{\chi p,n}^2$$

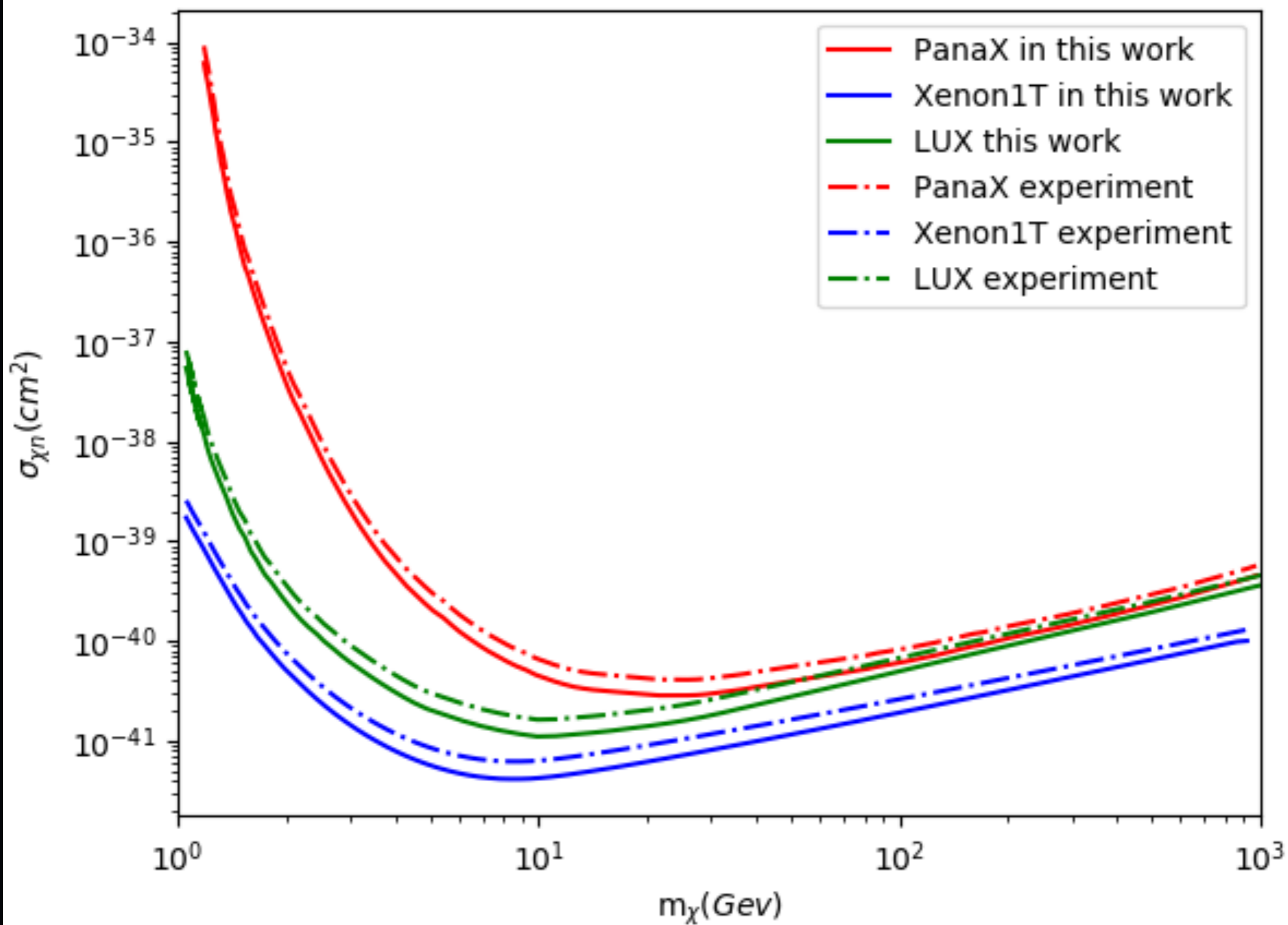
	$\langle S_p \rangle$	$\langle S_n \rangle$	$\langle S_p \rangle$	$\langle S_n \rangle$
Experiment	^{129}Xe		^{131}Xe	
Bonn A	0.028	0.359	-0.009	-0.227
Nijmegen II	0.0128	0.300	-0.012	-0.217

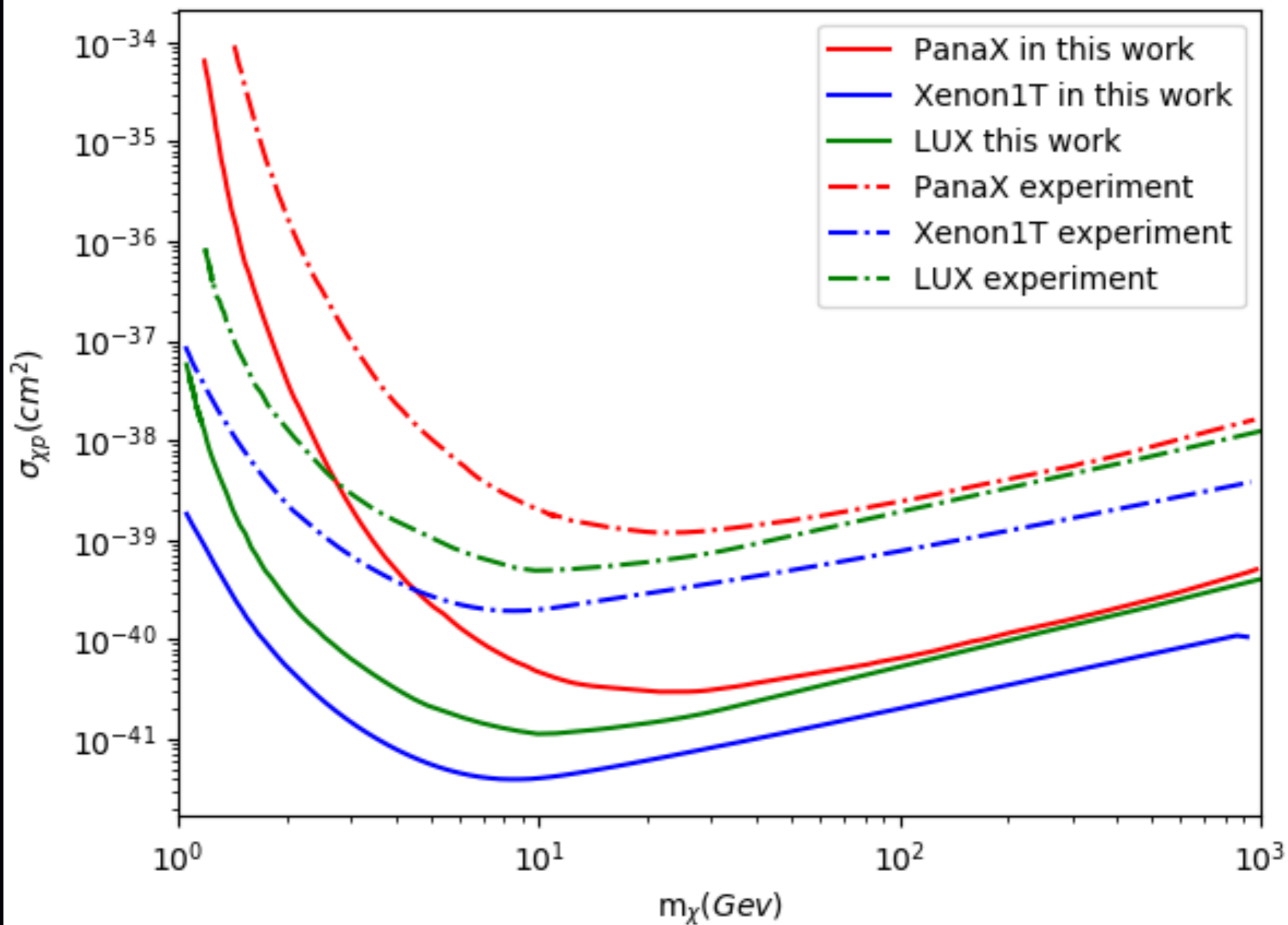
J. Menendez: Table 1 @ PhysRevD.86.103511

$$\sigma_{\chi p} = k(q^2) \times \sigma_{\chi n} + b(q^2)$$

Renewed Constrains on DM-Nucleon Interaction





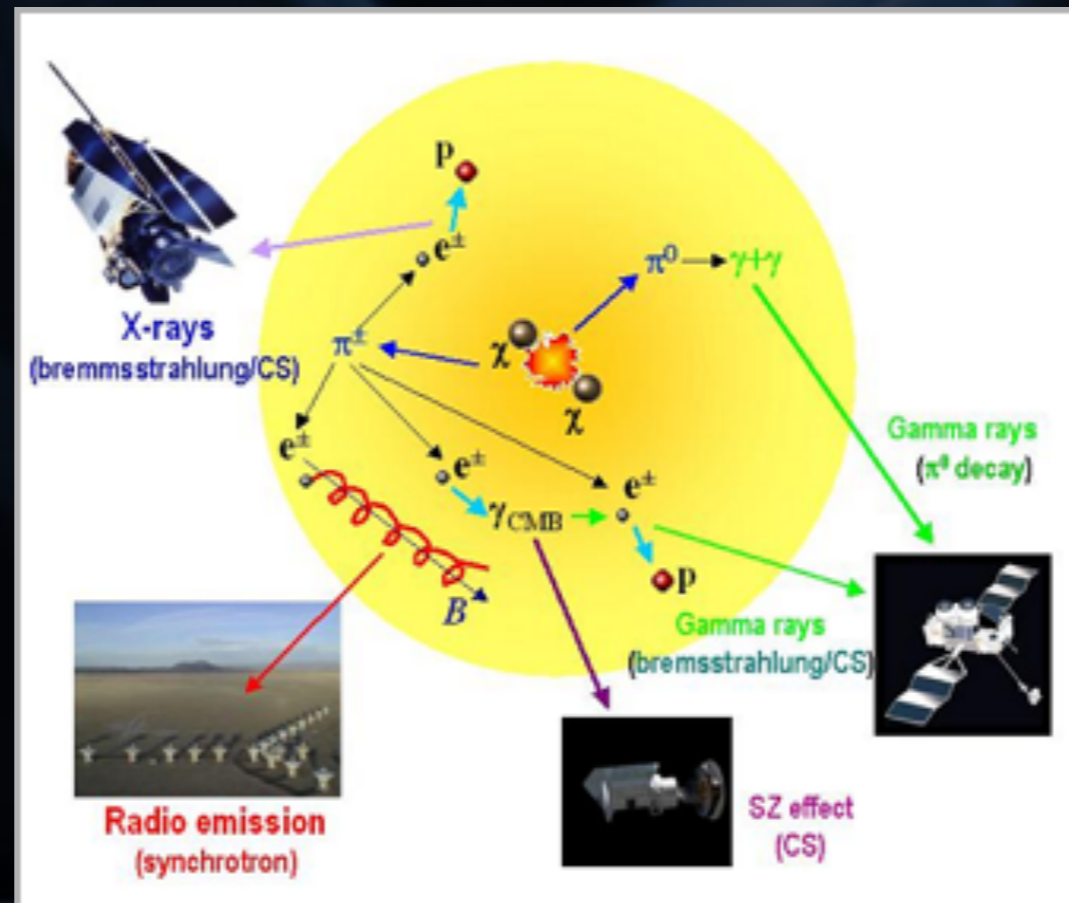


Summary

- Spin-Dependent Nucleon-DM Interaction
 - Nucleon Spin Structure evolution
 - $\sigma_{\chi p}^{SD} - \sigma_{\chi n}^{SD}$ Correlation evolution
 - Revised Constrains on DM parameter

Dark Matter Annihilation

- 1: Radio Emission in Dwarf Spheroidal Galaxies
- 2: Radio Emission in Dwarf Irregular Galaxies
- 3: Radio-FIR-Correlation: low luminosity end



Dark Matter Annihilation in LMC

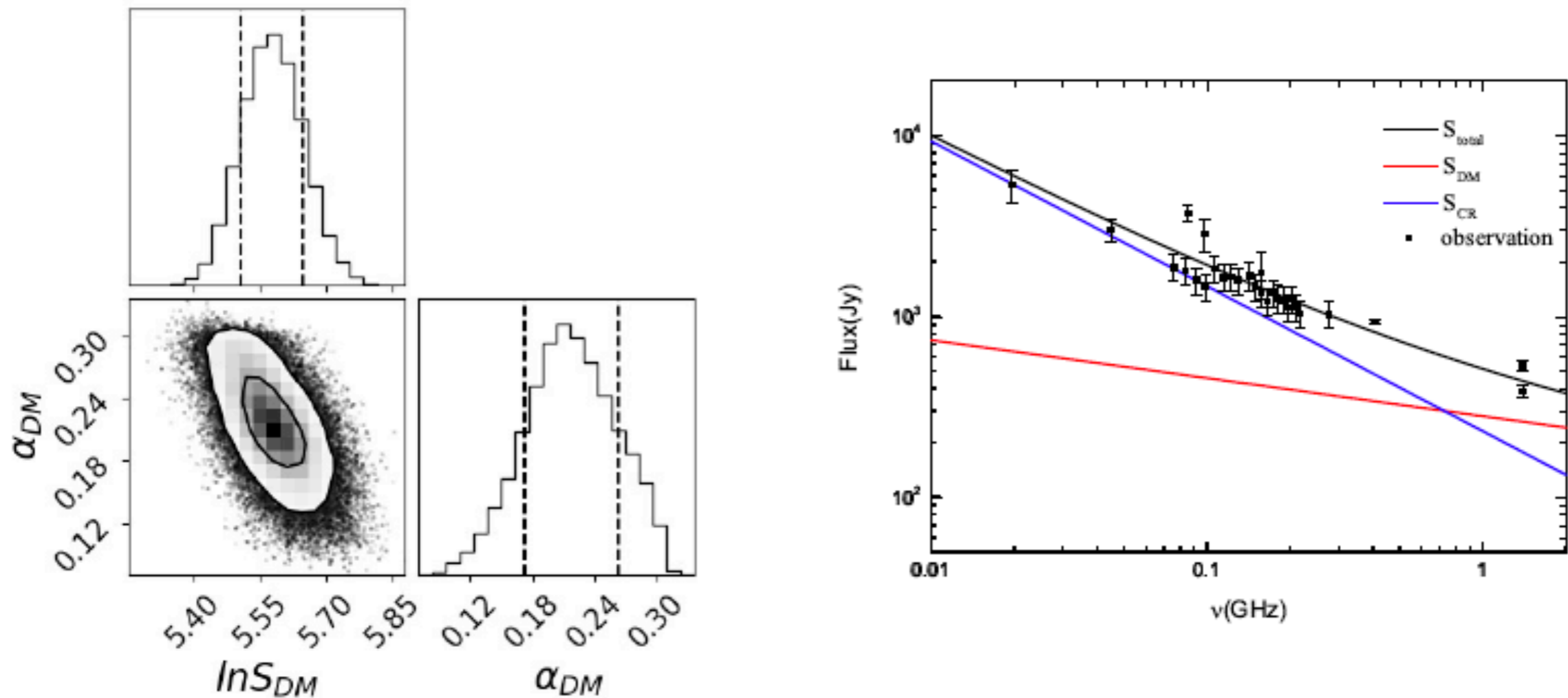


FIG. 1.— The left figure shows the contour of the probability distribution of radio flux with two free parameters. The right figure shows the radio flux versus frequency ν . The scatter points represent the observed data listed in Table 1. The blue line is synchrotron emission from CRs and the red line represents the allowed upper limit on synchrotron emission related to DM annihilation. The black line is the sum of these two components. The value of α_{CR} is 0.80.

Dark Matter Annihilation in LMC

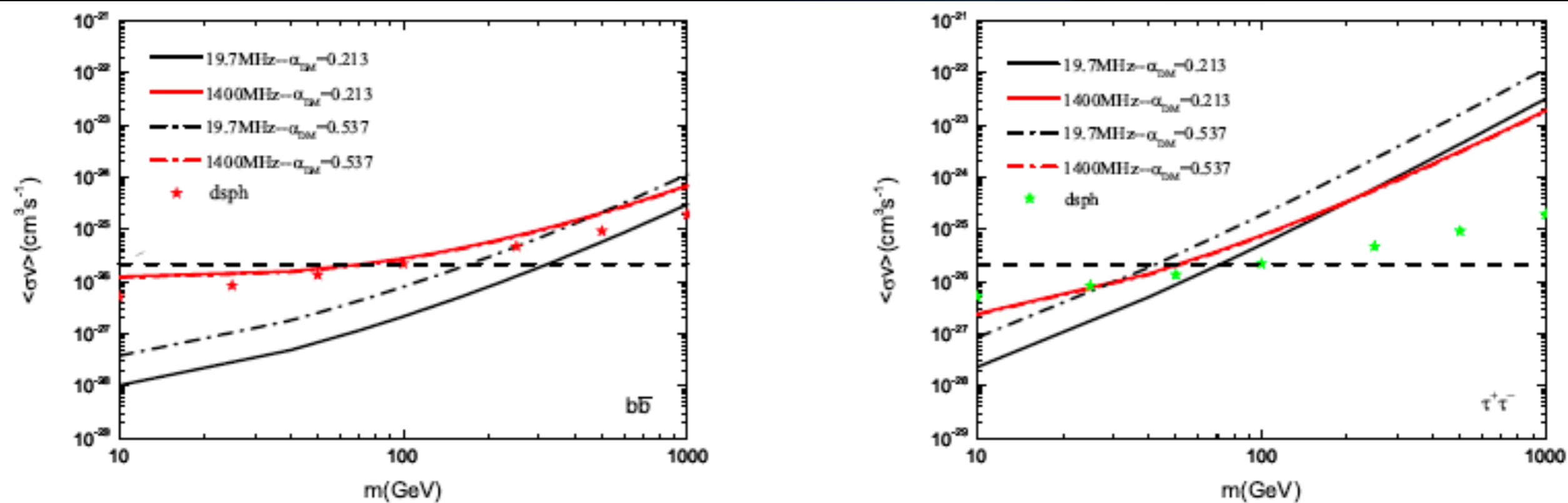
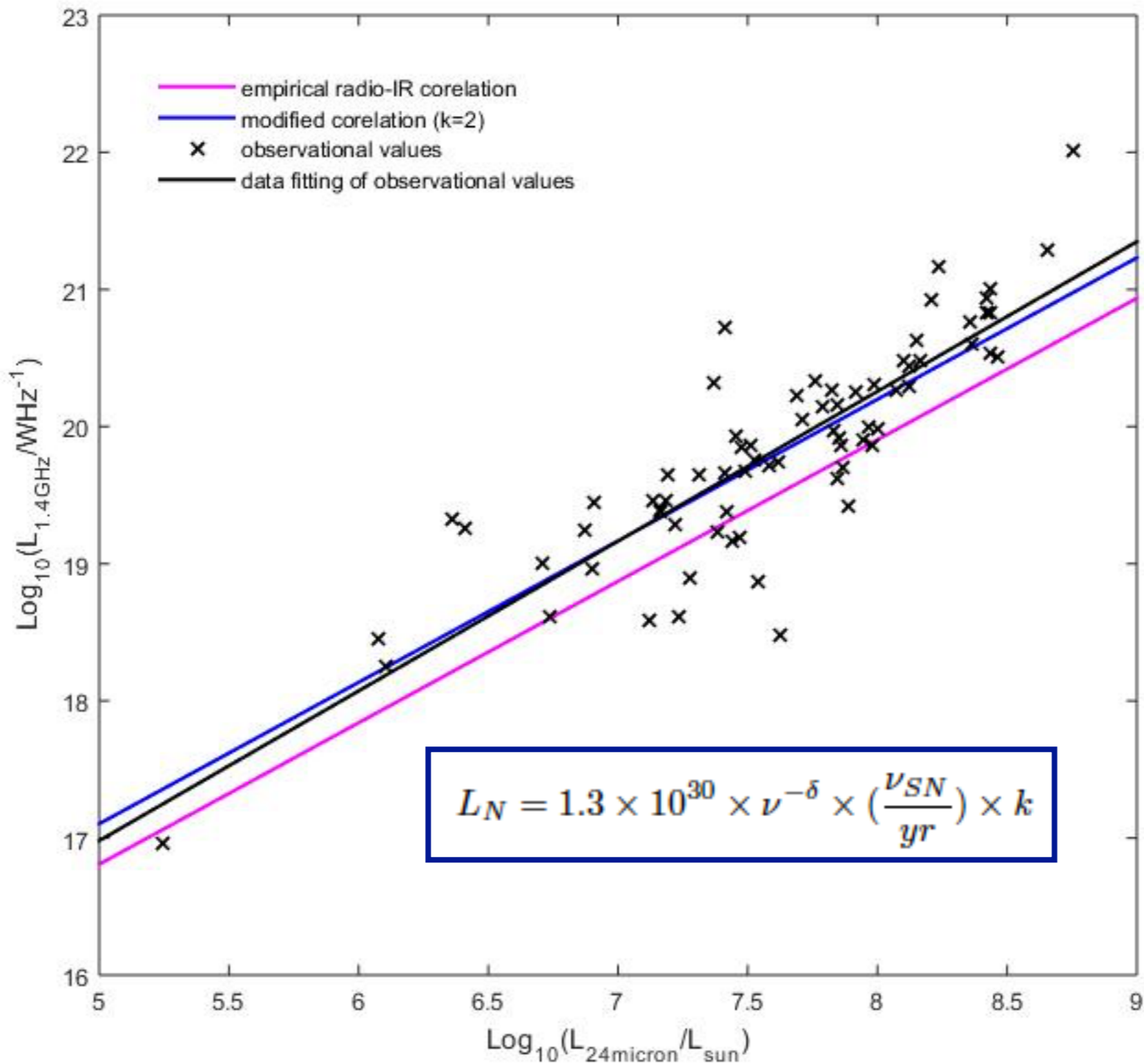


FIG. 5.— Constrains on m_χ and $\langle\sigma v\rangle$ parameter space for the $b\bar{b}$ annihilation channel assumed in left panel and $\tau^+\tau^-$ annihilation channel assumed in the right panel. Red lines represent constrains from 19.7 MHz and black lines from 1.4 GHz. Solid lines are accounted for $\alpha_{DM} = 0.213$ and dash-dotted lines for $\alpha_{DM} = 0.537$. Black dashed line represents annihilation cross section of thermal relics and stars are constrains derived from gamma ray observation on dSphs in Ackermann et al. (2015).

Radio-FIR-Correlation Correlation: 72 LSBG





廈門大學天文學系

Postdoctoral Fellow:

The Department of Astronomy at Xiamen University invites applicants for postdoctoral positions within the broad area of extragalactic astronomy and black hole accretion.

Applicants are expected to have completed the requirements for a PhD in astronomy, physics or related fields at the time of appointment, with a demonstrated track record of research. Preference will be given to candidates with research interests/experience in the following areas: accretion disks, X-ray binaries, gamma-ray burst, numerical simulations of structure formation, observational multi-wavelength observations of the formation and evolution of galaxies and AGN, the circumgalactic medium and the intergalactic medium.

The Astronomy Department consists of 10 faculties, 10 to 20 MS to PhD students, and has a very active research environment. We are a member of the Large Synoptic Survey Telescope (LSST), the Prime Focus Spectrograph (PFS) for Subaru Telescope, and we also have 10% share of observation time using the newly installed IFU at China's Lijiang Observatory.